ELECTRONIC SEISMOLOGIST

SRCMOD: An Online Database of Finite-Fault Rupture Models

by P. Martin Mai and K. K. S. Thingbaijam

INTRODUCTION

This contribution to the Electronic Seismologist presents the online SRCMOD database of finite-fault rupture models for past earthquakes, accessible at http://equake-rc.info/srcmod. Finite-fault earthquake source inversions have become a standard tool in seismological research. Using seismic data, these inversions image the spatiotemporal rupture evolution on one or more assumed fault segments. If geodetic data are used, the source inversions put constraints on the fault geometry and the static slip distribution (i.e., final displacements over the fault surfaces). Joint inversions, using a combination of available seismic, geodetic, and potentially other data, try to match all observations to develop a more comprehensive image of the rupture process. Some joint inversions use all data simultaneously, whereas others take an iterative approach wherein one set of observations is utilized to construct an initial (prior) model for subsequent inversions using other available data.

The field of finite-fault inversion was pioneered in the early 1980s (Olson and Apsel, 1982; Hartzell and Heaton, 1983). Subsequently, their method has been applied to numerous earthquakes (e.g., Hartzell, 1989; Hartzell *et al.*, 1991; Wald *et al.*, 1991; Hartzell and Langer, 1993; Wald *et al.*, 1993; Wald and Somerville, 1995), while simultaneously additional source-inversion strategies were developed and applied (e.g., Beroza and Spudich, 1988; Beroza, 1991; Hartzell and Lui, 1995; Hartzell *et al.*, 1996; Zeng and Anderson, 1996). It is beyond the scope of this article to provide a detailed review of source-inversion methods, their theoretical bases, implementations, and parameterizations; instead, we refer to Ide (2007) for a more comprehensive summary.

Finite-fault source inversions help to shape our understanding of the complexity of the earthquake rupture process. These source images provide information, albeit at rather low spatial resolution, of earthquake slip at depth, and potentially also on the temporal rupture evolution. Therefore, they represent an important resource for further research on the mechanics and kinematics of earthquake rupture processes. As such, they have a direct bearing on our understanding of earthquake source dynamics. For example, the seminal work of Heaton (1990) on the existence of slip pulses is based on the analysis of a set of finite-fault rupture models. Building on an early repository of slip models (then maintained by David Wald at the U.S. Geological Survey [USGS]), Somerville *et al.* (1999), Mai and Beroza (2000, 2002), and Lavallée *et al.* (2006) investigated slip heterogeneity and source-scaling relations of finite-fault rupture models and related their findings to coseismic stress change and near-source ground motion.

Mai (2004) expanded this early repository of slip models toward a more comprehensive finite-fault source-model database. The initial SRCMOD database was manually composed, consisted of about 80 rupture models for which individual HTML files were generated, and provided the first uniform rupture-model data format. Subsequently, this initial effort was technically improved and expanded to about 150 rupture models (Mai, 2007). The improved database sparked further research to investigate earthquake source complexity and earthquake scaling, also using complimentary data sets (Manighetti *et al.*, 2005; Causse *et al.*, 2010; Strasser *et al.*, 2010; Candela *et al.*, 2011). Using finite-fault rupture-model parameters, several authors studied the dynamics of the rupture process and associated ground motion of past earthquakes (e.g., Ide and Takeo, 1997; Zhang *et al.*, 2003; Tinti *et al.*, 2005, 2009; Mai *et al.*, 2006; Causse *et al.*, 2013). Other studies examined stress change on the fault (Ripperger and Mai, 2004), its relation to aftershock occurrence (Woessner *et al.*, 2006) and effects on stress triggering (e.g., Stein, 2003), and postseismic processes (e.g., Ergintav *et al.*, 2009). Detailed information on the kinematic rupture process also helps to shed light on the physics of rupture nucleation, propagation, and arrest (e.g., Mai *et al.*, 2005; Gabriel *et al.*, 2012) and allows the development of relations between slip asperities, temporal rupture properties, and geometrical source effects. These kinematic source parameters can then be related, for instance, to the occurrence of large near-field velocity pulses (Mena and Mai, 2011). Hence, investigating finite-fault rupture models with respect to their seismic radiation has immediate practical applications for earthquake-engineering purposes. Table 1 lists a small selection of published studies that utilized a previous version of the database.

In this contribution to the Electronic Seismologist, we present the expanded, updated, and refurbished SRCMOD database. Readily accessible at http://equake-rc.info/srcmod, the current version of SRCMOD currently offers source modelers, earthquake scientists, and any interested user open access to 300 earthquake rupture models, in a unified representation, published over the last 30 years. This online database also generates enhanced visibility of the research of authors who contribute their rupture models.

 doi: 10.1785/0220140077

Table 1
Selected Publications that Utilized the SRCMOD Database for Scientific Studies

Reference	Key Findings
Manighetti *et al.* (2005)	Earthquake slip distributions are roughly triangular, both along strike and down dip, and are mostly asymmetric.
Mai *et al.* (2005)	Earthquake hypocenters are located either within or close to regions of large-slip asperities; the scaling of slip asperity areas with seismic moment deviates from self-similarity behavior.
Woessner *et al.* (2006)	On-fault mainshock static shear-stress change does not correlate with aftershock locations over the rupture plane.
Song *et al.* (2009)	Earthquake slip correlates with temporal source parameters for rupture velocity, peak slip rate, and slip duration (rise time).
Hainzl *et al.* (2009)	Variability of Coulomb stress changes affects the correlation between predicted and observed changes in the rate of earthquake production.
Strasser *et al.* (2010)	New source-scaling relationships are presented, with focus on subduction-zone earthquakes.
Klinger (2010)	The thickness of seismogenic crust controls structural segmentation length of continental strike-slip earthquakes.
Causse *et al.* (2010)	Roughness degree of slip distributions correlates with the spatial distribution of peak ground acceleration.
Böse and Heaton (2010)	The authors calibrated their one-dimensional stochastic slip models with published finite-fault rupture models.
Gusev (2011)	One-point statistics of slip distributions are well approximated by a lognormal probability density function.
Candela *et al.* (2011)	Spatial correlations of slip distributions and fault topography roughness indicate identical self-affine properties.
Goda and Atkinson (2014)	Source-to-site distances evaluated from different intraevent finite-fault source models for megathrust subduction earthquakes greatly affect the interpreted ground motions.
Causse *et al.* (2013)	Dynamic source properties (e.g., fracture energy, static, and dynamic stress drop) tend to increase with earthquake magnitude.

In the following sections, we describe the technical aspects and implementation of SRCMOD as an online database and provide an overview of its contents and some general statistics of its current status. We then present a brief analysis on source-scaling properties using the current SRCMOD database. Potential further technical expansions and additional developments for expanded online access conclude this article.

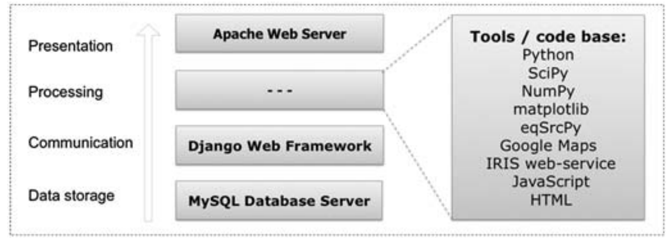

▲ **Figure 1.** A schematic description of components and software for the web development of the SRCMOD database.

TECHNICAL OVERVIEW

The SRCMOD website is built on a three-tier architecture comprised of client-side software (data presentation), server-side coding (data processing), and the back-end data storage. Figure 1 depicts a schematic presentation of components and software for the SRCMOD online database. We employ the Django web framework (Holovaty and Kaplan-Moss, 2009) in a LAMP implementation, in which "LAMP" stands for **L**inux operating system, **A**pache webserver, **M**ySQL database server, and **P**ython programing language. The server-side coding is implemented using Python and related packages, such as SciPy and NumPy (see Data and Resources). Specific additional functions for reading data files, file format conversions, and data processing are compiled into the *eqSrcPy* Python package (http://equake-rc.info/CERS-software; last accessed July 2014). Dynamic webpages are assembled within the Django template system.

For internal data archiving and access, we use both the file system and database management system. The primary data for the source models are stored in three different file formats: as MATLAB (www.mathworks.com/products/matlab; last accessed July 2014) structures (.mat files), as ASCII files that contain finite-source parameters (.fsp files), and as ASCII files that contain a comprehensive slip model (.slp files). Metadata for each rupture model, such as magnitude, seismic moment, hypocentral location, author and publication reference, and other relevant information are stored in the database management system, which is implemented with MySQL. In addition, we utilize the webservice provided by Incorporated Research Institutes for Seismology to obtain the Flinn–Engdahl region for the earthquake location (see Data and Resources). For displaying purposes, Google Maps API is used to generate maps that depict the geographical location of the rupture models (Figs. 2 and 3; see also Data and Resources).

The SRCMOD home page (Fig. 2) contains links to different components of the site. Any individual model can be accessed directly, using its unique identifier (*evTAG*), through http://equake-rc.info/srcmod/searchmodels/viewmodel/<evTAG>/. The 17-character *evTAG* string is constructed as "s

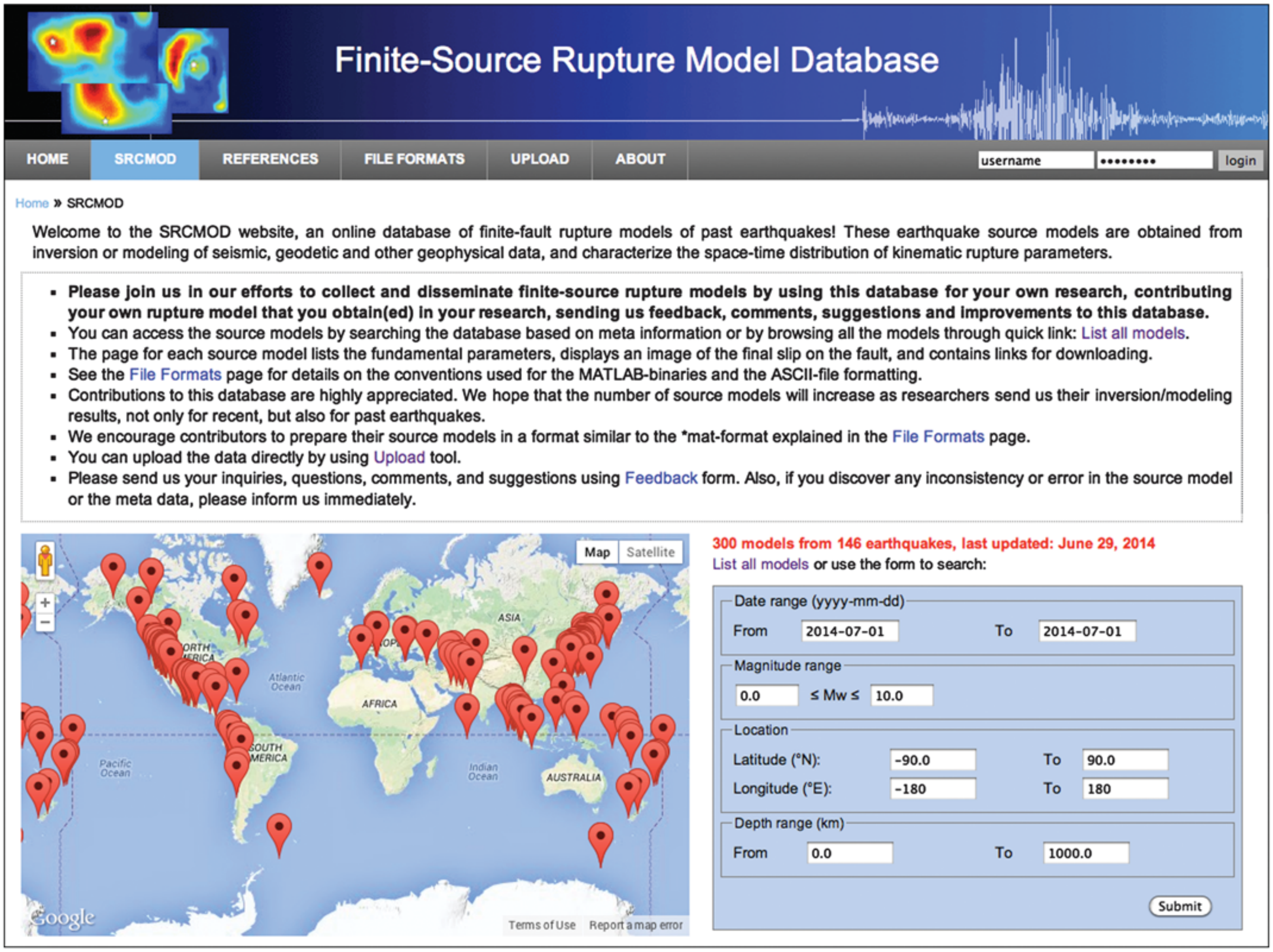

▲ **Figure 2.** The homepage of the SRCMOD finite-fault rupture-model database (both explained in the file-formats page,http://equake-rc.info/srcmod; last accessed July 2014). Links to different parts of the database appear in the gray area. The map displays the earthquake locations for which finite-fault models are available. The form on the bottom right of the page provides the user interface for searching the database according to specific criteria.

[YEAR][NAME][NO][AUTH]"; that is, use the starting letter "s," followed by the year of the earthquake, a six-character abbreviation to its name (based on location/name of the earthquake), a two-digit counter, and a four-letter abbreviation to the first author of the corresponding publication. A more general way to access rupture models is from a tabular listing of models. The listing can be obtained either for all models simultaneously or by database query using the available search option. Currently, the search tool allows rupture models to be filtered according to date of event, earthquake magnitude, epicentral location, and hypocentral depth.

The page for an individual rupture model (Fig. 3) displays fundamental source parameters and information related to the inversion parameterization, links to download the data in various formats, an image of the slip distribution on the fault surface with its 3D location, and a Google map depicting the geographical bounds of the model. The reference to the corresponding publication is linked to a compilation of references for all rupture models in the database. A detailed documentation on file formats and conventions is provided in separately linked pages accessible via the menu bar (Fig. 2). The implementation of the website ensures data integrity, such that data upload is allowed only to registered users authenticated by username and password. The user registration requires an email request, ensuring verification of the user, and his/her email address and affiliation. The data-upload tool currently accepts either .mat or .fsp format (both explained in the file-formats page, http://equake-rc.info/srcmod; last accessed July 2014).

DATA OVERVIEW AND SOURCE-MODEL VARIABILITY

As of June 2014, the SRCMOD database contains 300 models from 146 earthquakes of magnitudes ranging from M_w 4.1 to 9.2, spanning seven orders in seismic moment (1.6×10^{15} N·m $\le M_0 \le 7.7 \times 10^{22}$ N·m). The entire database

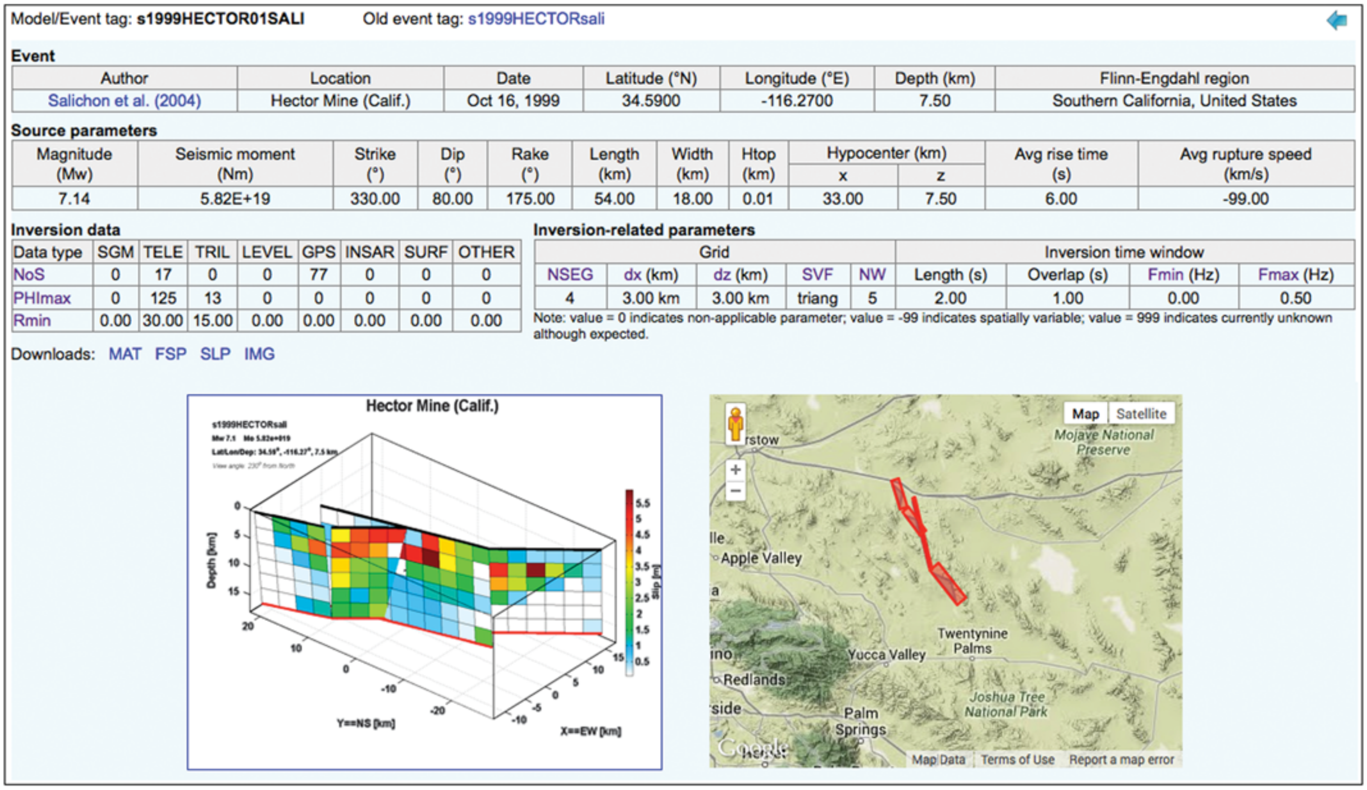

▲ **Figure 3.** An example page for an individual rupture model, available at http://equake-rc.info/srcmod/searchmodels/viewmodel/<evTAG>/, in which <evTAG> is the unique event identifier for each rupture model (in this case, <evTAG> is s1999HECTOR01SALI; see top-left corner). The tables provide event information and source parameters for this earthquake, as well as data and parameters related to how the inversion was carried out. A 3D view of the rupture, showing color-coded slip on the fault, and a map displaying the location of the rupture complete the event page. The selected example shows a rupture model for the 1999 M_w 7.1 Hector Mine earthquake (Salichon *et al.*, 2004).

represents an inhomogeneous global collection of earthquake rupture models—inhomogeneous in the sense of (1) earthquake location and thus tectonic province (interplate, intraplate, subduction), (2) faulting type, (3) available observations and data used in the source inversion, (4) inversion techniques applied, (5) model parameterizations selected and modeling choices made by the modelers, and (6) available rupture-model information provided by the authors. A finite-fault (also called kinematic) rupture model typically comprises several parameters, which include final slip, rise time (duration of slip), rupture-onset time, and rake (angle of slip direction). Not all source studies necessarily invert for all these parameters; instead, some parameters may be fixed/assumed in advance, depending on the data and the applied inversion strategy. The parameters may vary spatially and are defined at node points or subfaults that constitute the rupture surface. In case of inversions using seismic data, the source time function describes the temporal slip evolution on each point of the fault and is typically chosen using a simple parametric shape or as a linear combination of many elementary slip functions (so-called multi time-window inversions). The size of the subfaults (or spacing of node points) accounts for the nominal spatial resolution of the model, but typically the details of the rupture process are resolved at a larger scale as a result of the chosen smoothing constraints or regularization (to handle the ill-posed inversion problem) and the trade-off between parameters (Mai *et al.*, 2007; Monelli *et al*, 2009). The fault geometry considered may be simple (e.g., a single planar rupture surface with constant strike and dip) or complicated (e.g., including multiple segments of potentially various sizes, with varying strike and/or dip of individual segments).

Figure 4a depicts the number of rupture models annually published since 1983, as chronicled in the database. A significant growth in the source inversions can be seen over the last few years, most likely due to the increased availability of seismic and geodetic networks that allow detailed fault studies. Figure 4b indicates the predominance of large shallow (crustal) earthquakes in the database. The number of models is higher for earthquake magnitudes $M_w \geq 6.0$, but magnitudes in the M_w 7.0–8.0 range dominate, and hypocentral depths are generally below 25 km. We also see an abundance of models for reverse-faulting earthquakes (Fig. 4c) and that most source models in the database were inferred using teleseismic data (followed by inversions using a joint approach or strong-motion data).

Figures 2 and 4 illustrate the inhomogeneity of the SRCMOD database in terms of the six aspects listed above. Of course, increased availability of observational data (denser network coverage; near-real-time online data availability; harmonized data formats) and advanced source-inversion

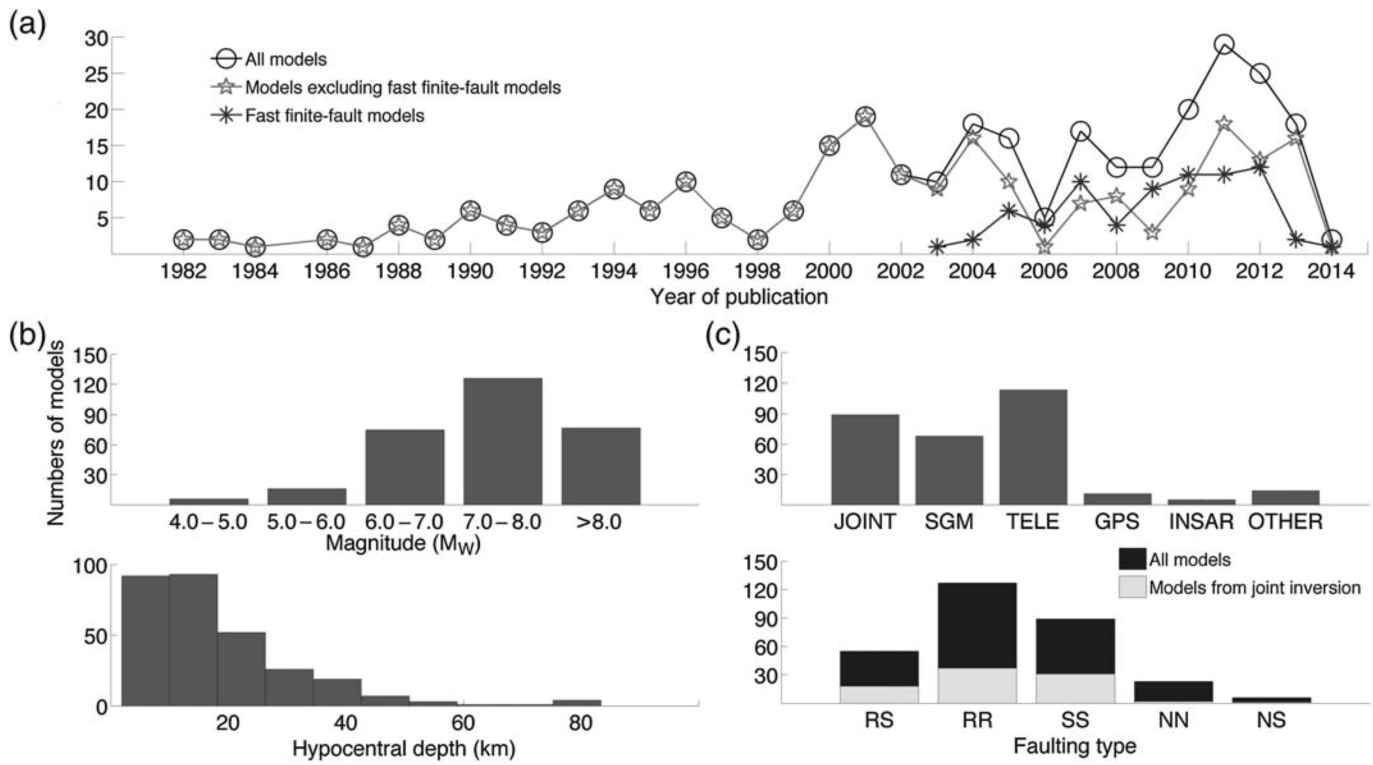

▲ **Figure 4.** The distribution of available rupture models in the SRCMOD database (status as of 30 June 2014): (a) time line of the number of rupture models published in the literature, (b) histograms of earthquake magnitudes (top) and hypocentral depths (bottom; two models for the 2013 Okhotsk Sea earthquake with the depth > 600 km are excluded), and (c) types of data used in the inversions (top) and faulting types of earthquakes in the database (bottom). JOINT, more than one data set is used for the inversion; SGM, strong ground-motion data; TELE, teleseismic recordings; GPS, Global Positioning System data; INSAR, Interferometric Synthetic Aperture Radar data; and OTHER, includes tsunami waveforms, leveling, trilateration, or other geophysical data. There are five different faulting styles: RS, reverse faulting with strike-slip components (or vice versa); RR, reverse faulting; SS, strike-slip faulting; NN, normal faulting; and NS, normal faulting with strike-slip components (or vice versa).

methods (from linearized multitime-window source inversion [Olson and Apsel, 1982; Hartzell and Heaton, 1983], to frequency-domain [Cotton and Campillo, 1995] and wavelet-domain inversion [Ji *et al.*, 2002] approaches, to nonlinear inversion techniques [e.g., Liu and Archuleta, 2004] and Bayesian inference [Monelli and Mai, 2008; Minson *et al.*, 2013; Razafindrakoto and Mai, 2014] contributed to the growth of the database and to the variability among the inferred rupture models. It is also important to note that so-called fast finite-fault inversions have become an almost routine analysis tool with which source models are generated in a semiautomated fashion within hours of a sizeable earthquake and then published online on institutional webpages.

Fast finite-fault models contribute significantly to the number of available source models. These online models are initially disseminated without peer-review processes, though a subset of them subsequently appears as journal publication (e.g., Hayes, 2011). Scientific projects or institutions that deliver online rupture models (not only fast finite-finite models) include finite-fault models at the USGS (http://earthquake.usgs.gov/earthquakes/eqinthenews/; last accessed July 2014), source models of large earthquakes at Caltech (http://www.tectonics.caltech.edu/slip_history/index.html; last accessed July 2014), database of big earthquakes at University of California–Santa Barbara (http://www.geol.ucsb.edu/faculty/ji/big_earthquakes/home.html; last accessed July 2014), and source process of recent earthquakes at University of Tsukuba (http://www.geol.tsukuba.ac.jp/~yagi-y/eng/earthquakes.html; last accessed July 2014).

The variety of source-inversion methods and available data contributes to the variability in rupture models. This is well documented in the current database, with 56 earthquakes for which multiple source models are available, out of which 31 earthquakes have more than two rupture models. Source models for the same event, such as available for the 2011 Tohoku, 2008 Wenchuan, 2004 Sumatra, 1999 İzmit, 1995 Kobe, or 1992 Landers earthquakes, exhibit significant intraevent variability. However, the nominal uncertainties in each of the sourceinversion studies are not well known. This has been pointed out previously (e.g., Beresnev, 2003) and can be understood in the context of the data used, the model parameterizations chosen, and the inversion techniques applied in such studies (Cohee and Beroza, 1994; Das and Suhadolc, 1996; Henry *et al.*, 2000; Graves and Wald, 2001; Delouis *et al.*, 2002; Yokota *et al.*,

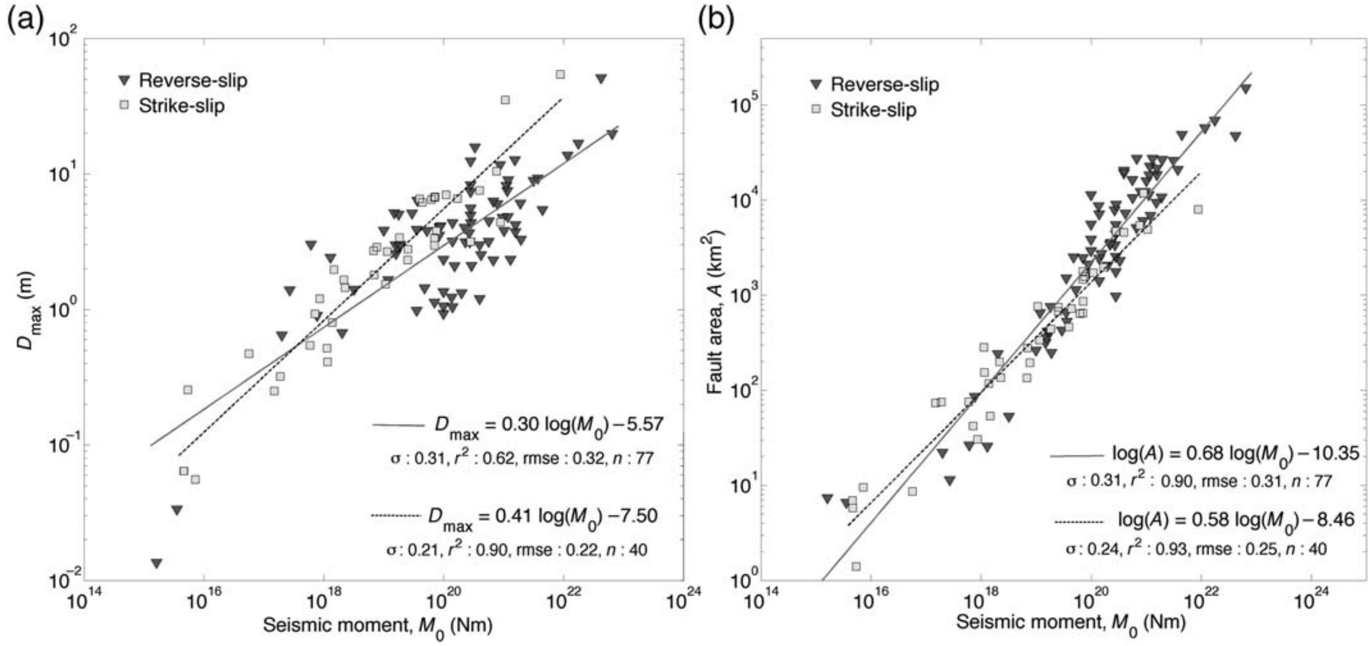

▲ **Figure 5.** General source-scaling behavior of rupture models in the SRCMOD database, displaying (a) maximum slip (D_{max}) on the fault plane and (b) fault area versus seismic moment. Strike-slip and reverse-slip ruptures are distinguished by filled inverted triangles and open squares, respectively. Effective source dimensions (Mai and Beroza, 2000), using median values when multiple rupture models exist for a single event, are shown. The straight lines mark the corresponding least-squares fit to these data. The solid and dashed lines correspond to the reverse-slip and strike-slip events, respectively. Resulting values for standard deviation (σ), coefficient of determination (r^2), root mean squared error (rmse), and number of data points (n) are stated below each scaling relation. Note the difference in scaling behavior of strike-slip and reverse-slip earthquakes. Interestingly, the estimated scaling does not depend on how effective source dimensions are computed (using the method of either Mai and Beroza, 2000, or Somerville *et al.*, 1999) or, for multiple rupture models for a single event, whether data points are treated independently or their mean or median values are used.

2011). Examples of particular interest are the rupture models for the recent $M_w \sim 9$ megathrust earthquakes in Sumatra (2004) and Japan (2011), for which compilations of source models are used for comparative analysis and subsequent research on their tsunamigenic properties (Shearer and Burgmann, 2010; Goda *et al.*, 2014; Tappin *et al.*, 2014). The fact that various source models for a specific earthquake exist allows for testing these models in terms of their predictive capabilities of available data, potentially those that have not been used to conduct respective inversion, and thus to obtain an independent posterior assessment of the model quality.

An assessment of intraevent model variability is important for better uncertainty quantification of earthquake source inversions, but also to extract the consistent features of the rupture process of a given earthquake. Such an analysis explores the variability (or consistency) of the models over a broad range of scales and examines various source parameters. Recognizing the justified skepticisms that these models may be far away from the true rupture process, they still collectively represent the current best state of knowledge on earthquake ruptures. Thus, it is important that any study using the database considers the possible sources of uncertainties associated with these models.

A recent effort to validate earthquake source-inversion methods is motivated by the intraevent source-model variability observed in the SRCMOD database. The Source Inversion Validation (SIV; http://equake-rc.info/siv; last accessed July 2014) project builds on a sequence of benchmark exercises of increasing complexity, with "true" solutions (because they are constructed as hypothetical earthquake ruptures), for which synthetic data are generated, disseminated, and then inverted by participating research teams to infer the known input model. Originally developed as a blind test of earthquake source inversion (Mai *et al.*, 2007), the ongoing SIV project expands these efforts toward rigorous uncertainty quantification in earthquake source studies (Page *et al.*, 2011).

SRCMOD DATA ANALYSIS: A BRIEF CASE STUDY

In the following, we present a brief case study on source-scaling behavior using the database, examining the behavior of maximum slip and the overall rupture area. The models are categorized by average faulting style, namely strike slip and reverse faulting (including oblique slip due to a component of strike-slip motion; Fig. 4). We consider all available source models for the analysis, without trying to (subjectively) select models that are deemed of higher quality (e.g., Causse *et al.*, 2010; Gusev, 2011; Causse *et al.*, 2013) or to subdivide the data according to other scientific criteria (e.g., Böse and Heaton, 2010; Strasser *et al.*, 2010; Goda and Atkinson, 2014). If several models are proposed for the same event by a single research group, we select their preferred source model. We exclude coarsely parameterized models with less than 50 subfaults due to statistical constraints on estimating effective source dimensions.

The earthquake source dimensions (i.e., length, width, or area) are generally estimated prior to the inversion from the spatial distribution of aftershocks. Rupture width is sometimes constrained by the thickness of the seismogenic crust; in other cases, source-scaling relationships are used to estimate fault-plane size. However, the inversion procedures commonly assume conservatively large source dimensions, so that the entire rupture can be accommodated. This leads to overestimated rupture sizes with small (even zero) displacements at the fault boundaries. Thus, it is necessary to trim the rupture model by eliminating superfluous small slips at the fault edges. In the present analysis, we compute effective fault dimensions based on the autocorrelation of the slip distribution, as suggested by Mai and Beroza (2000). Furthermore, in the case of multiple models for same event, we adopt median estimates to be representative of the central tendency of the model variability.

Figure 5 depicts log–log scatterplots of maximum slip (Fig. 5a) and rupture area (Fig. 5b) as a function of seismic moment, showing the estimates for strike-slip and reverse-slip earthquakes by different symbols. In the spirit of previous works on earthquake scaling relations (e.g., Wells and Coppersmith, 1994; Mai and Beroza, 2000; Hanks and Bakun, 2002, 2008; Strasser *et al.*, 2010), we fit a linear least-squares regression of the form $y = b\log_{10}(M_0) + a$ to the data points (solid and broken lines; corresponding scaling coefficients a and b are noted in the diagrams). Despite the large scatter of the data, distinct scaling properties can be observed. For instance, the maximum slip on the fault, D_{max}, appears to increase more rapidly with seismic moment for strike-slip earthquakes than for reverse-slip ruptures. In contrast, the rupture-area scaling shows self-similarity for dip-slip events (slope $b = 0.68$, which is approximately 2/3 as expected for self-similar scaling) but a significant smaller slope ($b = 0.58$) for strike-slip earthquakes.

Interestingly, these slopes are essentially independent of how the effective dimensions are computed (using either the approach of Mai and Beroza, 2000, or that of Somerville *et al.*, 1999), and also, whether all data points, or their mean or median, are considered when multiple rupture models exist for a single event. We also find that if we combine normal-faulting and reverse-faulting events into a single category (dip-slip events), its scaling is essentially the same as for reverse-slip events (slope $b = 0.68$; intercept $a = -10.09$ for area-moment scaling). These simple but robust observations suggest the breakdown of self-similarity for large strike-slip earthquakes, as conjectured previously (e.g., Romanowizc, 1992; Mai and Beroza, 2000).

The purpose of this contribution to the Electronic Seismologist is not a discussion on source-scaling properties and their implications for earthquake mechanics. Instead, we want to alert the reader to a number of important aspects of the SRCMOD database and the represented rupture models. Obviously, source models are sensitive to the data used to conduct the inversion, as well as to the chosen inversion methodology and parameterization. Hence, the apparently resolved spatial heterogeneity of the slip distribution depends on the data and the model parameterization. For instance, GPS and InSAR data have limited sensitivity to resolve deep slip but help to constrain seismic moment and geometry of the fault. Teleseismic data are strong in constraining seismic moment and overall rupture properties (that is, larger spatial scales) but have difficulties resolving temporal details. Strong-motion data are sensitive to rupture details on relatively fine space–time scales, but data distribution and wave-propagation effects strongly affect the slip inversion. Several studies suggests that a joint inversion of several data sets improves the stability of the inferred source model; however, this is at the expense of not being able to fit the individual data sets as well as in a separate inversion (e.g., Cohee and Beroza, 1994; Wald *et al.*, 1996; Wald and Graves, 2001; Delouis *et al.* 2002; Yokota *et al.*, 2011). In this context, we suggest that when utilizing rupture-model data for subsequent research, SRCMOD users make the following considerations to account (at least to some extent) for rupture-model uncertainty and the variability of multiple source models for a single earthquake.

1. Select source models according to how they were inferred (single data set; multiple data sets; joint inversion; inversion method; accuracy in Green's functions), and depending on which source-model information is used in the subsequent study.
2. If multiple models exist for a particular earthquake, assign appropriate weights to each model or compute an average representation of the models based on a measure of central tendency to avoid sampling bias due to the multiple models. The suitable measure of central tendency depends on the nature of the data; we adopt the median in the present analysis on source dimensions because the data distributions are often skewed.
3. The spatial sampling (i.e., subfault size) varies significantly across models in the database; for statistical analysis of rupture properties, this sampling variation needs to be accounted for, or models need to be selected accordingly.
4. As noted previously, models typically have overestimated source dimensions due to the larger fault area used for the inversion procedures. It may be necessary to trim the models, especially if the analysis involves rupture dimensions.
5. Classification of models according to style of faulting is not only important for tectonic and geodynamic considerations, but is also relevant for the mechanics of earthquakes. A style-of-faulting quantification can be achieved using the slip-weighted rake in each subfault to compute an overall rake angle. Some large earthquakes show considerable spatial rake variations, which in itself may lead to interesting earthquake mechanics and/or dynamic rupture interpretation.

FUTURE DEVELOPMENTS

We strive to continue developing the SRCMOD database by improving visualization capabilities, providing additional analysis tools, and increasing the number of rupture models. More flexible and interactive visualization of a slip distribution (or any other kinematic parameter) in 3D will facilitate a more comprehensive understanding of the rupture process, its geometry, and spatial complexity. The SRCMOD database, providing a unified representation of all source models, warrants a uniform yet flexible plotting approach. An improved visualization tool will address this plotting requirement for the user and additionally provide an immediate visual feedback during the data upload procedure.

To facilitate quantitative comparison of different source models, either for the same earthquake or for models of earthquakes of similar type, we plan to implement a variety of metrics that will be computed on the fly, like centroid location of the slip distribution (McGuire, 2004), effective source dimensions (Mai and Beroza, 2000), and statistical spatial comparison tests (Razafindrakoto *et al.*, 2014; Zhang *et al.*, 2014).

The current SRCMOD database contains only a subset of finite-fault rupture models that have been produced over time. Many more earthquakes have been studied using some form of finite-fault source inversion (or forward-modeling approach), and many such rupture models are published in the literature. To facilitate identification and acquisition of source models currently not in the database, we aim to create an online form to allow users/visitors to submit information related to existing but not-yet-available models. Future implementations may include support for direct submission of external file formats (e.g., the subfault format used by USGS) other than the SRCMOD formats in the data upload tool and provide application-oriented output file formats that can be used, for instance, for ground-motion simulations or in Coulomb stress modeling codes.

CONCLUDING REMARKS

The SRCMOD database (http://equake-rc.info/srcmod; last accessed July 2014) collects and disseminates finite-fault rupture models of earthquakes worldwide (currently containing 300 source models, magnitude range M_w 4.1–9.2). Rupture models are presented in several unified formats to expedite subsequent research in earthquake mechanics, dynamic rupture processes, and ground-motion simulations. The intraevent variability of the source models allows assessing the inherent uncertainty in earthquake source inversions that arises due to the nonuniqueness of the inverse problem, different inversion methods and parameterizations, and a variety of data and their processing for the inversion procedures. This database is anticipated to be a useful resource for seismological research. We encourage scientists across the globe to further contribute to the database and utilize it for research on the earthquake source processes.

DATA AND RESOURCES

Detailed information on the Python programming language and the open-source packages that use the language can be found at these websites: https://www.djangoproject.com, http://www.python.org, http://www.scipy.org, and http://matplotlib.org. The webservice provided by Incorporated Research Institutes for Seismology to obtain the Flinn–Engdahl region for the earthquake location can be found at http://service.iris.edu/irisws/flinnengdahl/2/. Google Maps is an online mapping technology provided by Google Inc.; more details can be found at https://developers.google.com/maps. All the websites were last accessed on April 2014.

ACKNOWLEDGMENTS

Foremost, we are indebted to all our colleagues who generously shared their published finite-fault rupture models with the SRCMOD database. Without their contributions, this database would not exist. Many source modelers and SRCMOD users sent comments and pointed out inconsistencies in the database (including E. Fielding, N. Poiata, F. Strasser, H. Sudhaus, E. Tinti, J. Donovan, and many others) and thus helped to improve this resource. We are very grateful for their feedback. X. Yang helped with literature surveys. The initial SRCMOD project received financial support from the European Commission Project RELIEF (EVG1-CT-2002-00069) and the Swiss Seismological Service at ETH Zürich,. The first version of the database was coded by F. Matter and F. Bethmann (both former students at ETH Zürich,). We are very thankful for continuous encouragement by J. Boatwright, M. Cocco, B. Ellsworth, D. Wald, and many others to build and maintain this database, in particular in the early stages of this project. We are grateful to J. Donovan and D. Wald for their constructive reviews of this article. This research was partially supported by the Southern California Earthquake Center (SCEC), which is funded by National Science Foundation (NSF) Cooperative Agreement EAR-1033462 and U.S. Geological Survey Cooperative Agreement G12AC20038. The SCEC contribution number for this paper is 1937. Research reported in this publication was supported by the King Abdullah University of Science and Technology (KAUST).

REFERENCES

Beresnev, I. A. (2003). Uncertainties in finite-fault slip inversions: To what extent to believe? (A critical review), *Bull. Seismol. Soc. Am.* **93,** 2445–2458.

Beroza, G. C. (1991). Near-source modeling of the Loma Prieta earthquake: Evidence for heterogeneous slip and implications for earthquake hazard, *Bull. Seismol. Soc. Am.* **81,** 1603–1621.

Beroza, G., and P. Spudich (1988). Linearized inversion for fault rupture behavior: Application to the 1984 Morgan Hill, California, earthquake, *J. Geophys. Res.* **93,** no. B6, doi: 10.1029/88JB01405.

Böse, M., and T. H. Heaton (2010). Probabilistic prediction of rupture length, slip and seismic ground motions for an ongoing rupture: Implications for early warning for large earthquakes, *Geophys. J. Int.* **183,** 1014–1030.

Candela, T., F. Renard, J. Schmittbuhl, M. Bouchon, and E. E. Brodsky (2011). Fault slip distribution and fault roughness, *Geophys. J. Int.* **187,** 959–968.

Causse, M., F. Cotton, and P. M. Mai (2010). Constraining the roughness degree of slip heterogeneity, *J. Geophys. Res.* **115,** no. B05304, doi: 10.1029/2009JB006747.

Causse, M., L. A. Dalguer, and P. M. Mai (2013). Variability of dynamic source parameters inferred from kinematic models of past earthquakes, *Geophys. J. Int.* **196,** 1754–1769, doi: 10.1093/gji/ggt478.

Cohee, B. P., and G. C. Beroza (1994). Slip distribution of the 1992 Landers earthquake and its implications for earthquake source mechanics, *Bull. Seismol. Soc. Am.* **84,** 692–712.

Cotton, F., and M. Campillo (1995). Inversion of strong ground motion in the frequency domain: Application to the 1992 Landers, California, earthquake, *J. Geophys. Res.* **100,** 3961–3975.

Das, S., and P. Suhadolc (1996). On the inverse problem for earthquake rupture: The Haskell-type source model, *J. Geophys. Res.* **101,** 5725–5738.

Delouis, B., D. Giardini, P. Lundgren, and J. Salichon (2002). Joint inversion of InSAR, GPS, teleseismic, and strong-motion data for the spatial and temporal distribution of earthquake slip: Application to the 1999 Izmit mainshock, *Bull. Seismol. Soc. Am.* **92,** 278–299.

Ergintav, S., S. McClusky, E. Hearn, R. Reilinger, R. Cakmak, T. Herring, H. Ozener, O. Lenk, and E. Tari (2009). Seven years of postseismic deformation following the 1999, $M = 7.4$ and $M = 7.2$, Izmit-Düzce, Turkey earthquake sequence, *J. Geophys. Res.* **114,** no. B7, doi: 10.1029/2008JB006021.

Gabriel, A.-A., J.-P. Ampuero, L. A. Dalguer, and P. M. Mai (2012). The transition of dynamic rupture styles in elastic media under velocity-weakening friction, *J. Geophys. Res.* **117,** no. B09311, doi: 10.1029/2012JB009468.

Goda, K., and G. M. Atkinson (2014). Variation of source-to-site distance for mega-thrust subduction earthquakes: Effects on ground motion prediction equations, *Earthq. Spectra* 845–866, doi: 10.1193/080512EQS254M.

Goda, K., P. M. Mai, T. Yasuda, and N. Mori (2014). Sensitivity of tsunami wave profile and inundation simulations to earthquake slip and fault geometry for the 2011 Tohoku earthquake, *Earth, Planets, Space* (unpublished manuscript).

Graves, R. W., and D. J. Wald (2001). Resolution analysis of finite fault source inversion using one- and three-dimensional Green's functions: 1. Strong motions, *J. Geophys. Res.* **06,** no. B5, 8745–8766.

Gusev, A. A. (2011). Statistics of the values of a normalized slip in the points of an earthquake fault, *Izvestiya Phys. Solid Earth* **47,** no. 3, 176–185.

Hainzl, S., B. Enescu, M. Cocco, J. Woessner, F. Catalli, R. Wang, and F. Roth (2009). Aftershock modeling based on uncertain stress calculations, *J. Geophys. Res.* **114,** no. B05309, doi: 10.1029/2008JB006011.

Hanks, T. C., and W. H. Bakun (2002). A bilinear source-scaling model for $\mathbf{M} - \log A$ observations of continental earthquakes, *Bull. Seismol. Soc. Am.* **92,** 1841–1846.

Hanks, T. C., and W. H. Bakun (2008). $\mathbf{M} - \log A$ observations for recent large earthquakes, *Bull. Seismol. Soc. Am.* **98,** 490–494.

Hartzell, S. H. (1989). Comparison of seismic waveform inversion results for the rupture history of a finite fault: Application to the 1986 North Palm Springs, California, earthquake, *J. Geophys. Res.* **94,** doi: 10.1029/89JB00321.

Hartzell, S. H., and T. H. Heaton (1983). Inversion of strong ground motion and teleseismic waveform data for the fault rupture history of the 1979 Imperial Valley, California, earthquake, *Bull. Seismol. Soc. Am.* **73,** 1553–1583.

Hartzell, S. H., and C. Langer (1993). Importance of model parameterization in finite fault inversions: Application to the 1974 M_w 8.0 Peru earthquake, *J. Geophys. Res.* **98,** no. B12, 22123–22134.

Hartzell, S. H., and P. Liu (1995). Determination of earthquake source parameters using a hybrid global search algorithm, *Bull. Seismol. Soc. Am.* **85,** 516–524.

Hartzell, S. H., P. Liu, and C. Mendoza (1996). The 1994 Northridge, California, earthquake: Investigation of rupture velocity, rise time, and high-frequency radiation, *J. Geophys. Res.* **101,** no. B9, 20091–20108.

Hartzell, S. H., G. S. Stewart, and C. Mendoza (1991). Comparison of L1 and L2 norms in a teleseismic waveform inversion for the slip history of the Loma Prieta, California, earthquake, *Bull. Seismol. Soc. Am.* **81,** 1518–1539.

Hayes, G. (2011). Rapid source characterization of the 2011 M_w 9.0 Off the Pacific Coast of Tohoku earthquake, *Earth Planets Space*, **63,** 529–534.

Heaton, T. H. (1990). Evidence for and implications of self-healing pulses of slip in earthquake rupture, *Phys. Earth Planet. Int.* **64,** 1–20.

Henry, C., S. Das, and J. H. Woodhouse (2000). The great March 25, 1998, Antarctic Plate earthquake: Moment tensor and rupture history, *J. Geophys. Res.* **105,** 16097–16118.

Holovaty, A., and J. Kaplan-Moss (2009). *The Definitive Guide To Django: Web Development Done Right*, Second Ed., APress, Berkeley, California.

Ide, S. (2007). Slip inversion, in *Treatise on Geophysics*, in Earthquake Seismology, H. Kanamori (Series Editor), Vol. 4, Elsevier, Amsterdam, The Netherlands, ISBN: 978-0-444-51932-0, 193–224.

Ide, S., and M. Takeo (1997). Determination of constitutive relations of fault slip based on seismic wave analysis, *J. Geophys. Res.* **102,** 27,379–27,391.

Ji, C., D. J. Wald, and D. V. Helmberger (2002). Source description of the 1999 Hector Mine, California earthquake; Part I: Wavelet domain inversion theory and resolution analysis, *Bull. Seismol. Soc. Am.* **92,** 1192–1207.

Klinger, Y. (2010). Relation between continental strike-slip earthquake segmentation and thickness of the crust, *J. Geophys. Res.* **115,** no. B07306, doi: 10.1029/2009JB006550.

Lavallée, D., P. Liu, and R. J. Archuleta (2006). Stochastic model of heterogeneity in earthquake slip spatial distributions, *Geophys. J. Int.* **165,** 622–640.

Liu, P., and R. J. Archuleta (2004). A new nonlinear finite fault inversion with three-dimensional Green's functions: Application to the 1989 Loma Prieta, California, earthquake, *J. Geophys. Res.* **109,** no. B02318, doi: 10.1029/2003JB002625.

Mai, P. M. (2004). SRCMOD: A database of finite-source rupture models, *Annual Meeting of the Southern California Earthquake Center (SCEC)*, Palm Springs, California, 19–22 September 2004, 19–23.

Mai, P. M. (2007). SRCMOD: A database of finite source rupture models, http://www.seismo.ethz.ch/srcmod (last accessed December 2013).

Mai, P. M., and G. C. Beroza (2000). Source-scaling properties from finite-fault rupture models, *Bull. Seismol. Soc. Am.* **90,** 604–615.

Mai, P. M., and G. C. Beroza (2002). A spatial random-field model to characterize complexity in earthquake slip, *J. Geophys. Res.* **107,** doi: 10.1029/2001JB000588.

Mai, P. M., P. Spudich, and J. Boatwright (2005). Hypocenter locations in finite-source rupture models, *Bull. Seismol. Soc. Am.* **95,** 965–980.

Mai, P. M., J. Burjanek, B. Delouis, G. Festa, C. Francois-Holden, D. Monelli, T. Uchide, and J. Zahradnik (2007). Earthquake source inversion blind test: Initial results and further developments. *Eos Trans. AGU* **88,** no. 52, (Fall Meet. Suppl.), Abstract S53C-08.

Mai, P. M., P. Somerville, A. Pitarka, L. Dalguer, H. Miyake, G. Beroza, S.-G. Song, and K. Irikura (2006). Fracture-energy scaling in dynamic rupture models of past earthquakes, *Earthquakes: Radiated Energy and the Physics of Faulting, American Geophysical Monograph* **170,** 283–294, doi: 10.1029/170GM28.

Manighetti, I., M. Campillo, C. Sammis, P. M. Mai, and G. King (2005). Evidence for self-similar, triangular slip distributions on earthquakes: Implications for earthquake and fault mechanics, *J. Geophys. Res.* **110,** no. B05302, doi: 10.1029/2004JB003174.

McGuire, J. J. (2004). Estimating finite source properties of small earthquake ruptures, *Bull. Seismol. Soc. Am.* **94,** 377–393.

Mena, B., and P. M. Mai (2011). Selection and quantification of near-fault velocity pulses owing to source directivity, *Georisk* **5,** 25–43.

Minson, S. E., M. Simons, and J. L. Beck (2013). Bayesian inversion for finite fault earthquake source models I—theory and algorithm, *Geophys. J. Int.* doi: 10.1093/gji/ggt180.

Monelli, D., and P. M. Mai (2008). Bayesian inference of kinematic earthquake rupture parameters through fitting of strong motion data, *Geophys. J. Int.* **173,** 220–232, doi: 10.1111/j.1365-246X.2008.03733.x.

Monelli, D., P. M. Mai, S. Jonsson, and D. Giardini (2009). Bayesian imaging of the 2000 Western Tottori (Japan) earthquake through fitting of strong motion and GPS data, *Geophys. J. Int.* doi: 10.1111/j.1365-246X.2008.03943.x.

Olson, A. H., and R. J. Apsel (1982). Finite faults and inverse theory with applications to the 1979 Imperial Valley earthquake, *Bull. Seismol. Soc. Am.* **72,** 1969–2001.

Page, M., P. M. Mai, and D. Schorlemmer (2011). Testing earthquake source inversion methodologies, *Eos Trans. AGU* **92,** no. 9, 75.

Razafindrakoto, H. N. T., and P. M. Mai (2014). Uncertainty in earthquake source imaging due to variations in source time function and Earth structure, *Bull. Seismol. Soc. Am.* **104,** 855–874, doi: 10.1785/0120130195.

Razafindrakoto, H. N. T., L. Zhang, K. K. S. Thingbaijam, P. M. Mai, and M. G. Genton (2014). An embedding method to quantify rupture model variation, *Geophys. Res. Abstr.*, **16,** EGU2014-3920, 2014 EGU General Assembly.

Ripperger, J., and P. M. Mai (2004). Fast computation of static stress changes on 2D faults from final slip distributions, *Geophys. Res. Lett.* **31,** L18610, doi: 10.1029/2004GL020594.

Romanowicz, B. (1992). Strike-slip earthquakes on quasi-vertical transcurrent faults: Inferences for general scaling relations, *Geophys. Res. Lett.* **19,** 481–484.

Salichon, J., P. Lundgren, B. Delouis, and D. Giardini (2004). Slip history of the 16 October 1999 M_w 7.1 Hector Mine earthquake (California) from the inversion of InSAR, GPS, and teleseismic data, *Bull. Seismol. Soc. Am.* **94,** 2015–2027.

Shearer, P. M., and R. Bürgmann (2010). Lessons learned from the 2004 Sumatra-Andaman megathrust rupture, *Ann. Rev. Earth Planet. Sci.* **38,** doi: 10.1146/annurev-earth-040809-152537.

Somerville, P., K. Irikura, R. Graves, S. Sawada, D. Wald, N. Abrahamson, Y. Iwasaki, T. Kagawa, N. Smith, and A. Kowada (1999). Characterizing crustal earthquake slip models for the prediction of strong ground motion, *Seismol. Res. Lett.* **70,** 59–80.

Song, S. G., A. Pitarka, and P. Somerville (2009). Exploring spatial coherence between earthquake source parameters, *Bull. Seismol. Soc. Am.* **99,** 2564–2571.

Stein, R. S. (2003). Earthquake conversations, *Sci. Am.* **288,** no. 1, 72–79.

Strasser, F. O., M. C. Arango, and J. J. Bommer (2010). Scaling of the source dimensions of interface and intraslab subduction-zone earthquakes with moment magnitude. *Seismol. Res. Lett.* **81,** no. 6, 941–950.

Tappin, D. R., S. T. Grilli, J. C. Harris, R. J. Geller, T. Masterlark, J. T. Kirby, F. Shi, G. Ma, K. K. S. Thingbaijam, and P. M. Mai (2014). Did a submarine landslide contribute to the 2011 Tohoku tsunami? *Marine Geol.* (unpublished manuscript).

Tinti, E., M. Cocco, E. Fukuyama, and A. Piatanesi (2009). Dependence of slip weakening distance (D_c) on final slip during dynamic rupture of earthquakes, *Geophys. J. Int.* **177,** 1205–1220.

Tinti, E., P. Spudich, and M. Cocco (2005). Earthquake fracture energy inferred from kinematic rupture models on extended faults, *J. Geophys. Res.* **110,** no. B12303, doi: 10.1029/2005JB003644.

Wald, D. J., and R. W. Graves (2001). Resolution analysis of finite fault source inversion using one-and three-dimensional Green's functions: 2. Combining seismic and geodetic data, *J. Geophys. Res.* **106,** 8767–8788.

Wald, D. J., and P. G. Somerville (1995). Variable-slip rupture model of the great 1923 Kanto, Japan, earthquake: Geodetic and body-waveform analysis, *Bull. Seismol. Soc. Am.* **85,** 159–177.

Wald, D. J., T. H. Heaton, and K. W. Hudnut (1996). The slip history of the 1994 Northridge, California, earthquake determined from strong-motion, teleseismic, GPS, and leveling data, *Bull. Seismol. Soc. Am.* **86,** S49–S70.

Wald, D. J., D. V. Helmberger, and T. H. Heaton (1991). Rupture model of the 1989 Loma Prieta earthquake from the inversion of strong-motion and broadband teleseismic data, *Bull. Seismol. Soc. Am.* **81,** 1540–1572.

Wald, D. J., H. Kanamori, D. V. Helmberger, and T. H. Heaton (1993). Source study of the 1906 San Francisco earthquake, *Bull. Seismol. Soc. Am.* **83,** 981–1019.

Wells, D. L., and K. J. Coppersmith (1994). New empirical relationships among magnitude, rupture length, rupture width, rupture area, and surface displacement, *Bull. Seismol. Soc. Am.* **84,** 974–1002.

Woessner, J., D. Schorlemmer, S. Wiemer, and P. M. Mai (2006). Spatial correlation of aftershock locations and on-fault main shock properties, *J. Geophys. Res.* **111,** no. B08301, doi: 10.1029/2005JB003961.

Yokota, Y., K. Koketsu, Y. Fujii, K. Satake, S. Sakai, M. Shinohara, and T. Kanazawa (2011). Joint inversion of strong motion, teleseismic, geodetic, and tsunami datasets for the rupture process of the 2011 Tohoku earthquake, *Geophys. Res. Lett.* **38,** L00G21, doi: 10.1029/2011GL050098.

Zeng, Y., and J. G. Anderson (1996). A composite source model of the 1994 Northridge earthquake using genetic algorithms, *Bull. Seismol. Soc. Am.* **86,** S71–S83.

Zhang, L., P. M. Mai, K. K. S. Thingbaijam, H. N. T. Razafindrakoto, and M. G. Genton (2014). Comparing earthquake slip models with the spatial prediction comparison test, *Geophys. J. Int.* (unpublished manuscript).

Zhang, W. B., T. Iwata, and K. Irikura (2003). Heterogeneous distribution of the dynamic source parameters of the 1999 Chi-Chi, Taiwan, earthquake, *J. Geophys. Res.* **108,** 2232–2245.

P. Martin Mai
K. K. S. Thingbaijam
King Abdullah University of Science and Technology
Division of Physical Sciences and Engineering
Thuwal 23955-6900
Kingdom of Saudi Arabia
martin.mai@kaust.edu.sa

Published Online 1 October 2014